Supplementary Materials

On the Measure of the Heat Transfer Performance of RANS Turbulence Models in Single Round Jet Impingement

Sebastian Gurgul and Elzbieta Fornalik-Wajs*

1. Geometry and boundary conditions

1.1. Geometry

Table S1 presents the dimensions of the computational domain for all the cases analyzed.

Table S1. Geometry dimensions for all analyzed *H/D* values.

H/D	*H*, m	*D*, m	*Inlet length*, m	x_{max}, m
1	0.02	0.02	0.02	0.17
2	0.04			
4	0.08			
6	0.12			

1.2. Boundary conditions

The boundary conditions are as follows:

- Inlet
  - Boundary condition type: *velocity-inlet*. Inlet profiles for all analyzed cases are available in the repository [48];
  - Fully developed profile with uniform temperature of 293 K;
- Inlet wall
  - Boundary condition type: *wall*;
  - No-slip, adiabatic (heat flux 0 W/m^2);
- Bottom wall (Heated wall)
  - Boundary condition type: *wall*;
  - No-slip, constant heat flux 1000 W/m^2;
- Domain exit (right surface)
  - Boundary condition type: *pressure-outlet;*
  - Gauge pressure equals 0 Pa (operating pressure is 101,325 Pa). The total backflow temperature is set to be the same as the inlet temperature (293 K);
- Left surface (axis)
  - Rotational symmetry axis for 2D axisymmetric model;
- Top surface
  - Boundary condition type: *pressure-outlet;*
  - Gauge pressure equals 0 Pa (Operating pressure is 101,325 Pa). The total temperature is set to the same as the inlet temperature (293 K).

Studies described in [13] showed that only small values of the *H/D* ratio (below 1) type of top surface boundary condition pressure-outlet (unconfined)/wall (confined) influence the Nusselt number distribution at the heated wall. Figure S1 presents an influence of the boundary condition of the top surface on the Nusselt number distribution. The maximum observable differences are equal to 2% of the value of the Nusselt number. In the

presented study, values of H/D equaling 1 and higher are considered; therefore, a *pressure-outlet* was selected as a boundary condition.

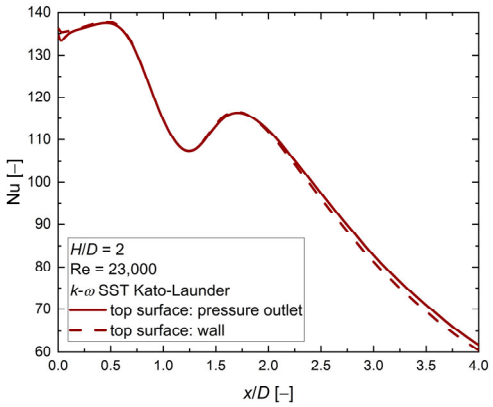

Figure S1. Influence of the type of boundary condition of the top surface on the Nusselt number distribution. *k-ω* SST Kato-Launder, H/D = 2, D = 0.02 m, Re = 23,000.

1.3. Influence of inlet diameter

Figure S2 shows the size of the influence of the inlet diameter on the Nusselt number distribution in the study for three selected turbulence models. Numerically obtained results showed no influence. However, according to Lee et al. [11], the diameter size might be a source of discrepancies in the distribution of the Nusselt number in experimental studies due to the lack of control of an inlet velocity profile.

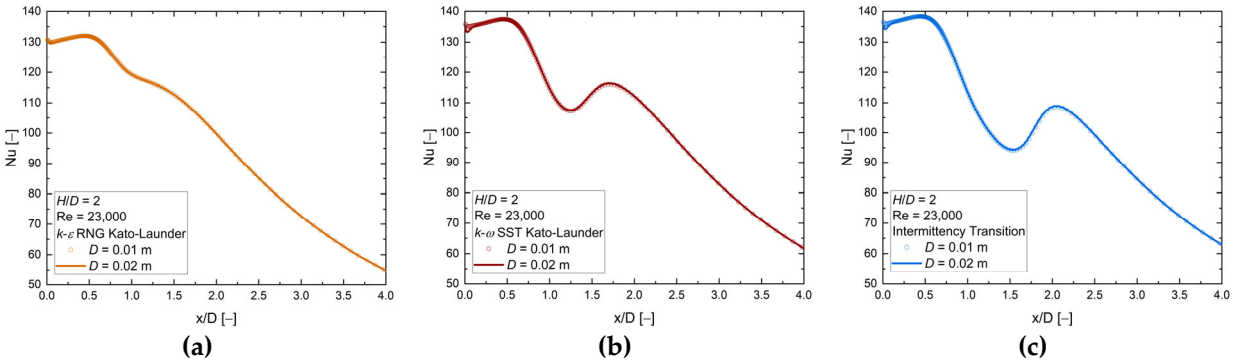

Figure S2. Influence of an inlet diameter on the Nusselt number distribution. H/D = 2, D = 0.01 m and D = 0.02 m, Re = 23,000. (a) *k-ε* RNG Kato-Launder, (b) *k-ω* SST Kato-Launer, (c) Intermittency Transition.

1.4. Influence of inlet profile

Figure S3, Figure S4, and Figure S5 show the influence of the inlet profile on the Nusselt number distribution for three turbulence models at H/D = 2 and Re = 23,000. Five inlet profiles have been tested: the flat profile, 2D, 5D, 10D (which means how long the inlet channel was—in inlet diameters, before fluid entered the domain), and the fully developed. The flat and fully developed profile limits the Nusselt number distribution for all three tested turbulence models. These findings correspond to [13] [16] [47].

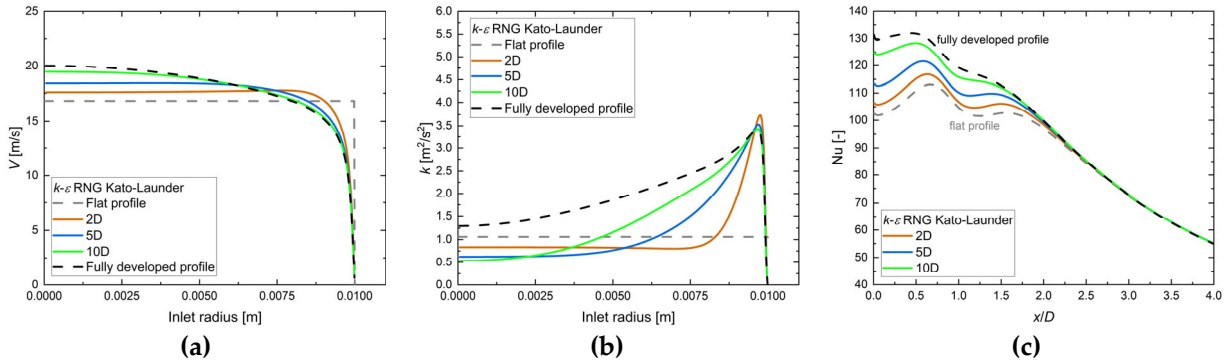

Figure S3. Influence of (a) a velocity inlet profile H/D = 2, D = 0.02 m, Re = 23,000, k-ε RNG Kato-Launder, on (b) the kinetic turbulence energy profile, (c) the Nusselt number distribution.

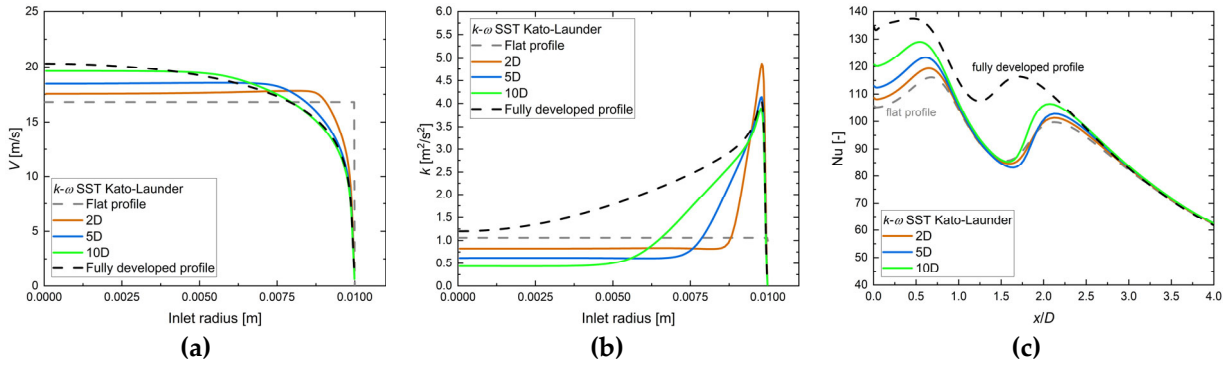

Figure S4. Influence of (a) a velocity inlet profile H/D = 2, D = 0.02 m, Re = 23,000, k-ω SST Kato-Launder, on (b) the kinetic turbulence energy profile, (c) the Nusselt number distribution.

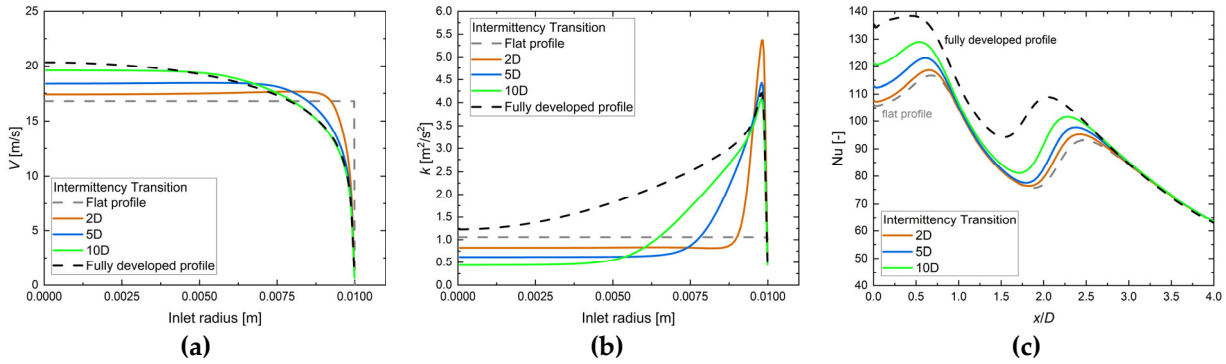

Figure S5. Influence of (a) a velocity inlet profile H/D = 2, D = 0.02 m, Re = 23,000, Intermittency Transition, on (b) the kinetic turbulence energy profile, (c) the Nusselt number distribution.

2. Mesh

Figures S6–S9 present mesh sizing for four geometrical configurations: Figure S6 for H/D = 1, Figure S7 for H/D = 2, Figure S8 for H/D = 4, and Figure S9 for H/D = 6.

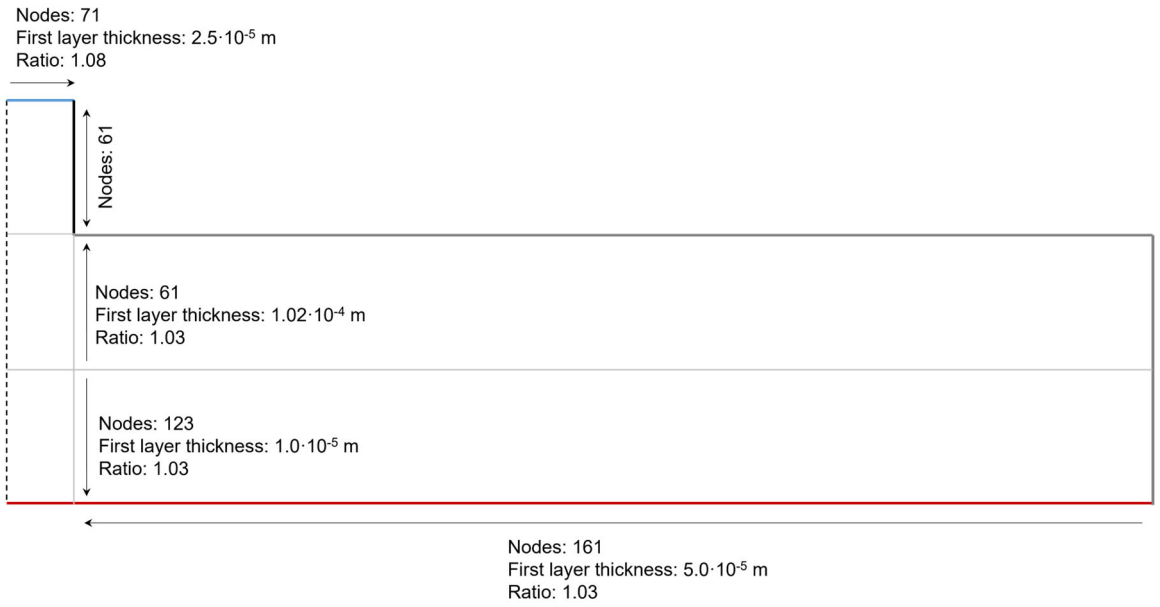

Figure S6. Mesh details, $H/D = 1$, the total number of cells = 46,060.

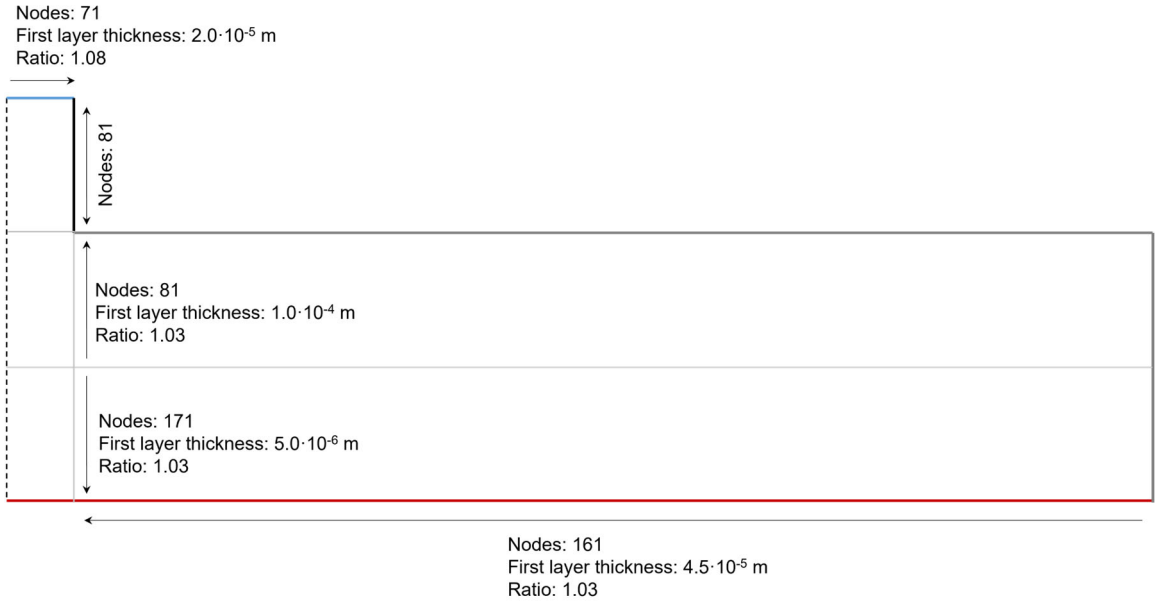

Figure S7. Mesh details, $H/D = 2$, the total number of cells = 63,100.

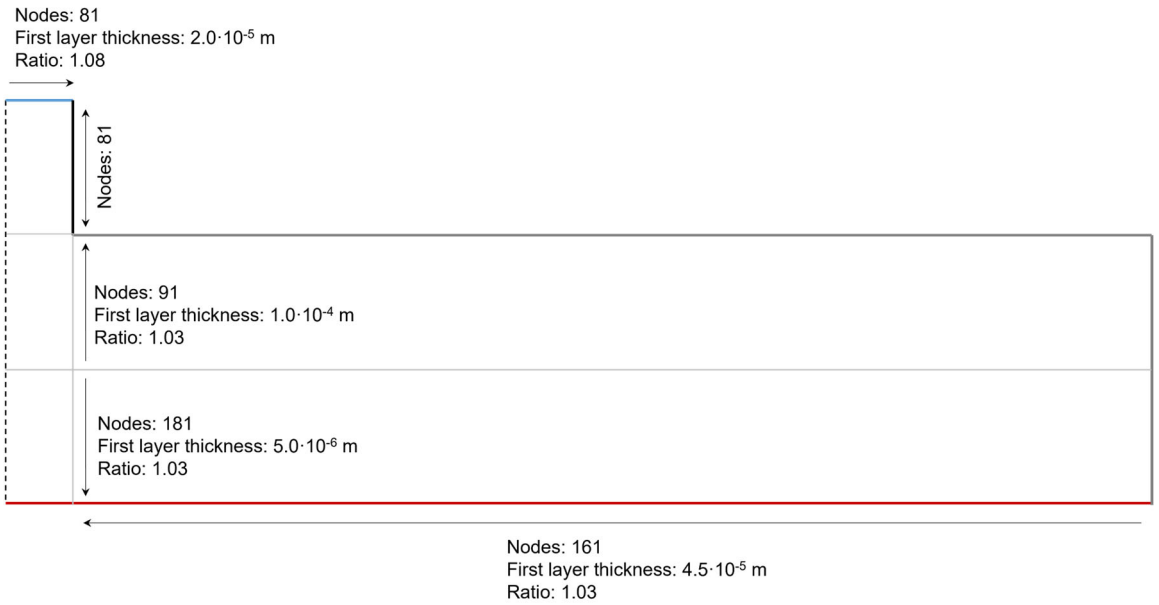

Figure S8. Mesh details, H/D = 4, the total number of cells = 71,200.

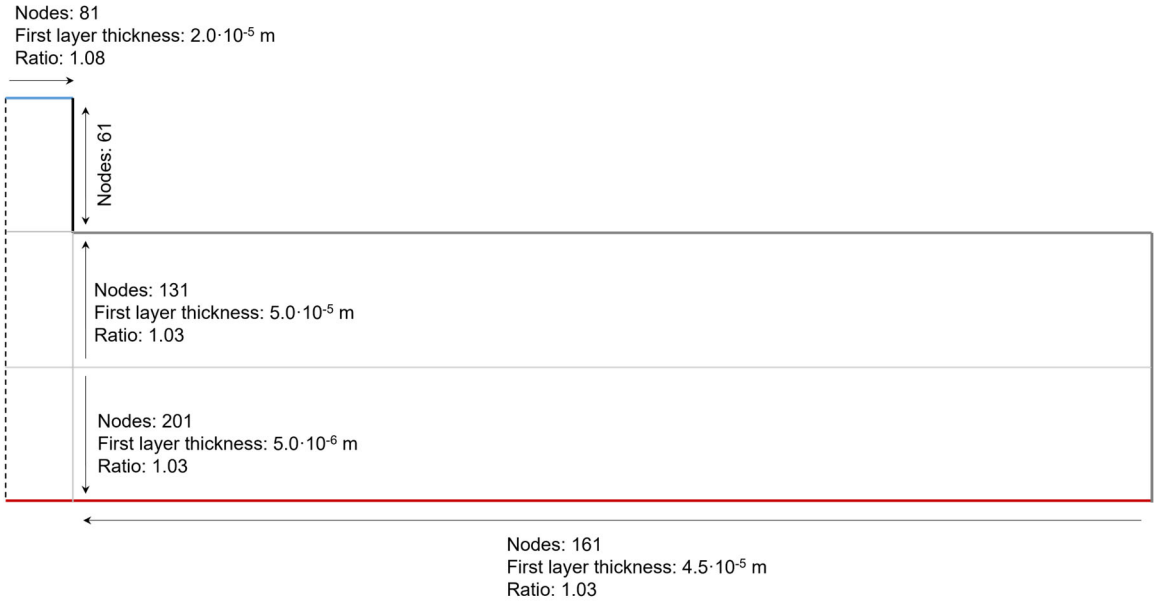

Figure S9. Mesh details, H/D = 6, the total number of cells = 80,100.

3. Convergence and residuals

Stabilization of the average Nusselt number on the heated surface was selected as a convergence criterion, with residual values equal to 10^{-6}. For the k-ω SST Kato-Launder turbulence model, H/D = 2, Re = 23,000 case, stabilization of the average Nusselt number at the heated surface and residuals values equaling 10^{-6} were achieved after 6000 iterations. After 12,000–14,000 iterations, residuals achieved stabilization. Plots of the average Nusselt number and residuals for the case H/D = 2, D = 0.02 m, Re = 23,000, and k-ω SST Kato-Launder are presented in Figure 10. The average Nusselt number values at the heated wall for 2000 iterations are shown in Figure 10 (a), and in Figure 10 (b) for 14,000 iterations. Analogically, the residuals for 2000 iterations are shown in Figure 10 (c), and in Figure 10 (d) for 14,000 iterations. The dashed lines represent the development of particular flow structures, which is described in more detail.

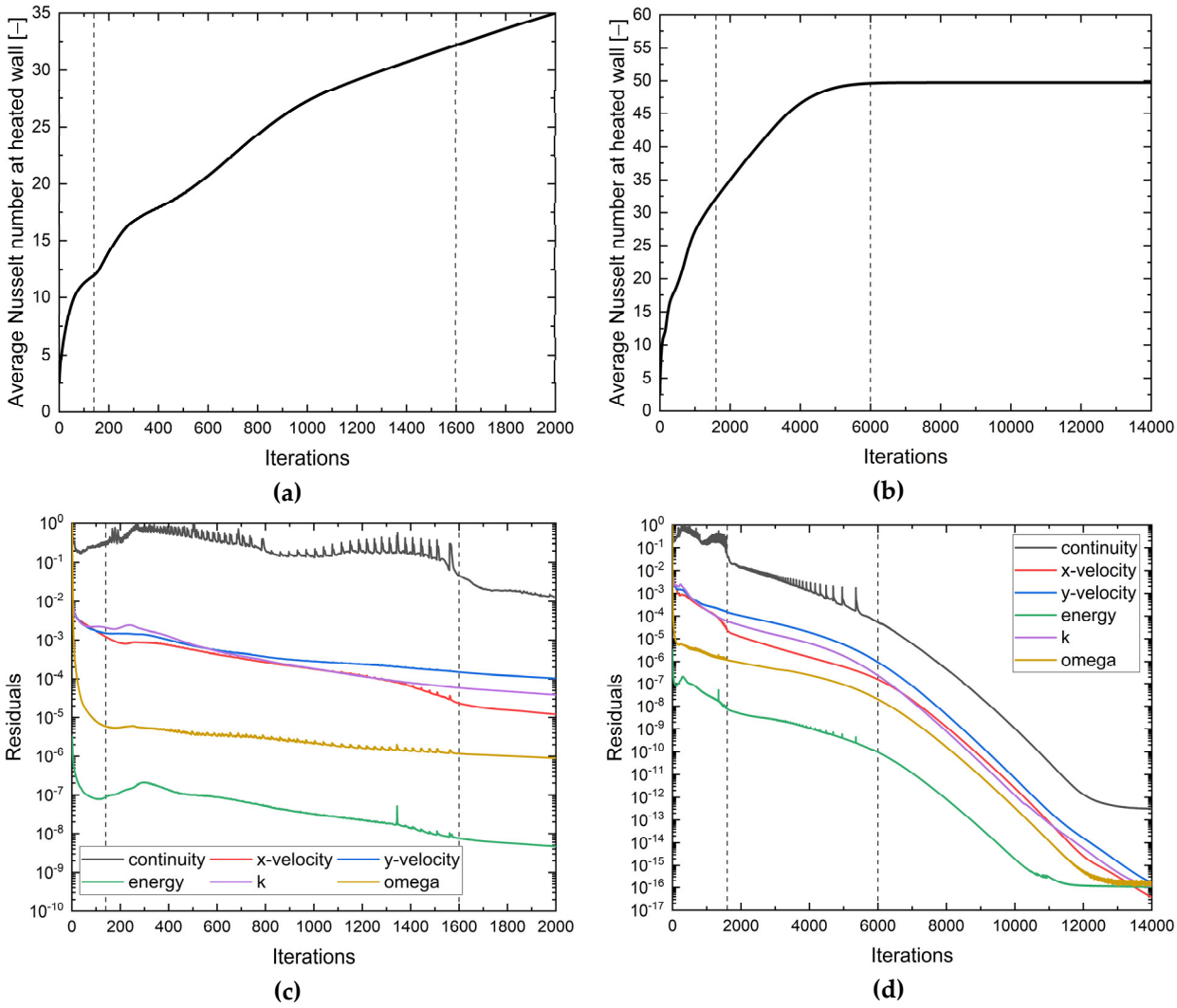

Figure S10. Monitor of the average Nusselt number at heated surface, (a) until 2000 iterations, (b) until 14,000 iterations; the residuals, (c) until 2000 iterations, (d) until 14,000 iterations. H/D = 2, D = 0.02 m, Re = 23,000, k-ω SST Kato-Launder.

Figures S10 (a) and S10 (c) show the first 2000 iterations. A closer look at the residuals (c) and average Nusselt number monitor (a) reveals that a few interesting things are happening during the steady-state calculations:

- 1–140 iterations: free jet is developing;
- ~140 iteration: the jet is starting to impinge on the heated surface, which can be seen as the inflection point on the average Nusselt number monitor;
- 140–1600 iterations: residual oscillations correlate with the development of wall jet and movement of the large vortex structure towards the outlet of the computational domain;
- 1600–6000 iterations: the vortex structure is starting to escape the computational domain, oscillations in residuals are still visible;
- > 6000 iterations: the solution process starts to stabilize.

4. Jet hydrodynamics

4.1. Velocity and turbulent kinetic energy profiles

Figure S11 compares dimensionless velocity profiles obtained numerically on four vertical lines from the axis with the experimental results [49]. The comparison shows good agreement with the experimental data. The differences between the k-ε RNG Kato-Launder turbulence model and the others are visible, but the velocity profiles obtained using the k-ω SST Kato-Launder and Intermittency Transition turbulence models are almost the

same. This observation does not explain the differences in the Nusselt number distributions for the same case. This explanation comes from comparisons in Figure S12, where the kinetic energy distribution is shown. The turbulent kinetic energy plots calculated using the *k-ω* SST Kato-Launder and Intermittency Transition turbulence models are similar, but some discrepancies can be observed. Figure S12 (c) shows those differences at $x/D = 1$, where the Nusselt number distribution begins to split between the results determined using the *k-ω* SST Kato-Launder and Intermittency Transition turbulence models. An analysis of velocity profiles alone is insufficient to understand the jet impingement phenomenon.

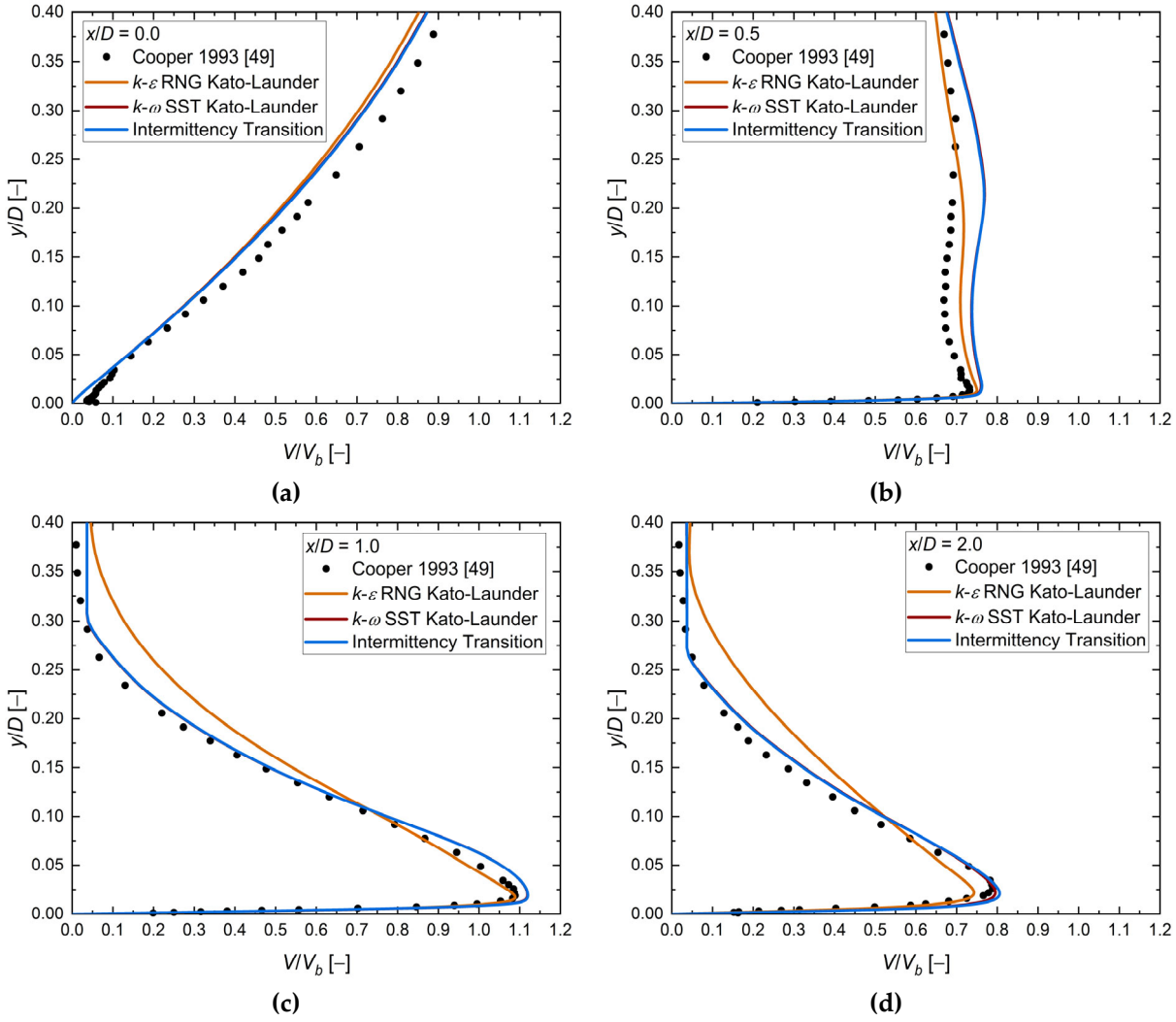

Figure S11. Comparison of numerically obtained velocity profiles with experimental data [49], (a) $x/D = 0.0$, (b) $x/D = 0.5$, (c) $x/D = 1.0$, (d) $x/D = 2.0$. $H/D = 2$, $D = 0.02$ m, Re = 23,000, $V_b = 16.8$ m/s. y — vertical distance from the heated wall ($y/D = 0$ — heated wall), x — horizontal distance from axis ($x/D = 0$ — axis).

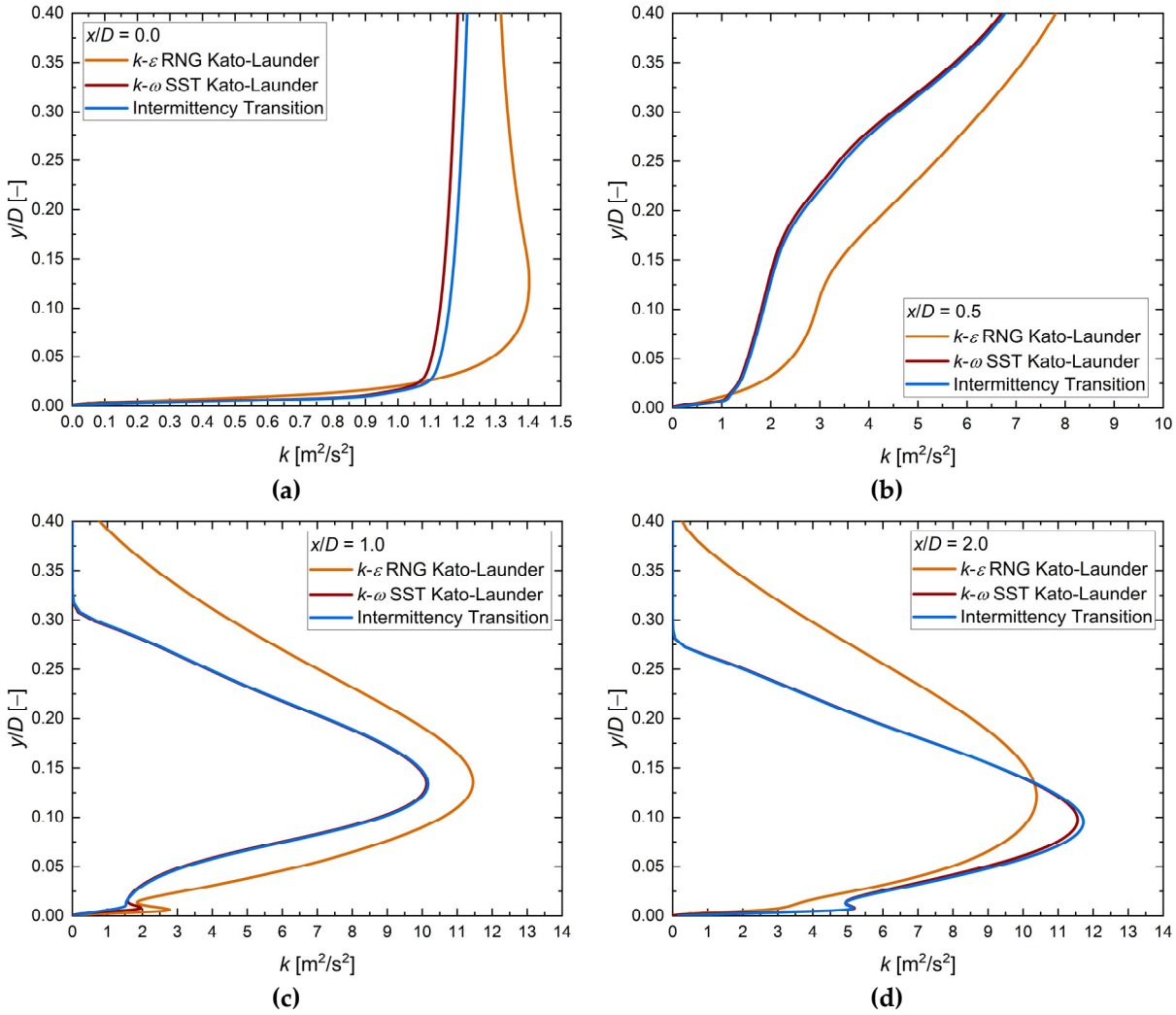

Figure S12. Comparison of numerically obtained turbulent kinetic energy k profiles, (a) x/D = 0.0, (b) x/D = 0.5, (c) x/D = 1.0, (d) x/D = 2.0. H/D = 2, D = 0.02 m, Re = 23,000. y — vertical distance from the heated wall (y/D = 0 — heated wall), x — horizontal distance from axis (x/D = 0 — axis).

4.2. Jet velocity and turbulent kinetic energy development

Figure S13 and Figure S14 demonstrate the evolution of velocity and turbulent kinetic energy profiles of a jet entering the fluid domain. The figures present the results for six levels representing the distance from the top to bottom. These six levels are at y/D = 2.0, 1.5, 1.0, 0.5, 0.25 and 0.005. The level at y/D = 2.0 corresponds to the inlet of the air, while y/D = 0.005 level is very close to the heated wall. The jet core is visible in Figures S13 and S14 (a) – (e). The similarities between profiles obtained using the k-ω SST Kato-Launder and Intermittency Transition turbulence models can be observed, and the discrepancies between those two and k-ε RNG Kato-Launder turbulence model, in both Figures S13 and S14 (a) – (e). Such a comparison shows no correlation between the velocity/turbulent kinetic energy profile and the Nusselt number distribution. Therefore, an analysis of these profiles near the heated wall is required. In Figure S13 (e) and Figure S14 (e) this link between the mentioned profiles and the Nusselt number distribution can be seen. An intersection of profiles obtained using the k-ε RNG Kato-Launder with k-ω SST Kato-Launder and Intermittency Transition turbulence models, the same as splitting and reconnecting profiles calculated using the k-ω SST Kato-Launder and Intermittency Transition, correlates with the Nusselt number distribution.

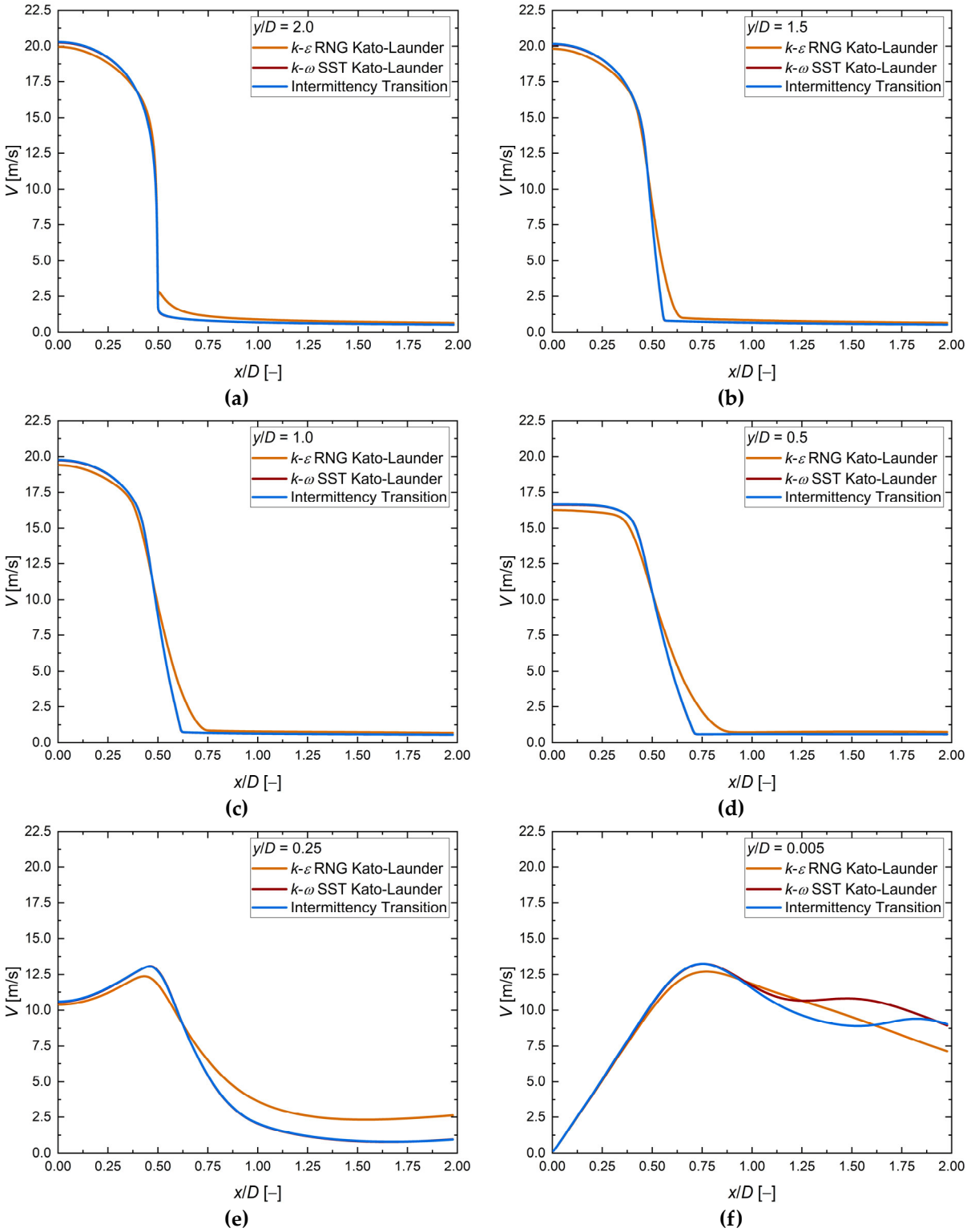

Figure S13. Velocity profile development. H/D = 2, D = 0.02 m, Re = 23,000, (a) y/D = 2.0, (b) y/D = 1.5, (c) y/D = 1.0, (d) y/D = 0.5, (e) y/D = 0.25, (f) y/D = 0.005. y — vertical distance from the heated wall (y/D = 0 — heated wall, y/D = 2.0 — exit of the inlet channel), x — horizontal distance from axis (x/D = 0 — axis).

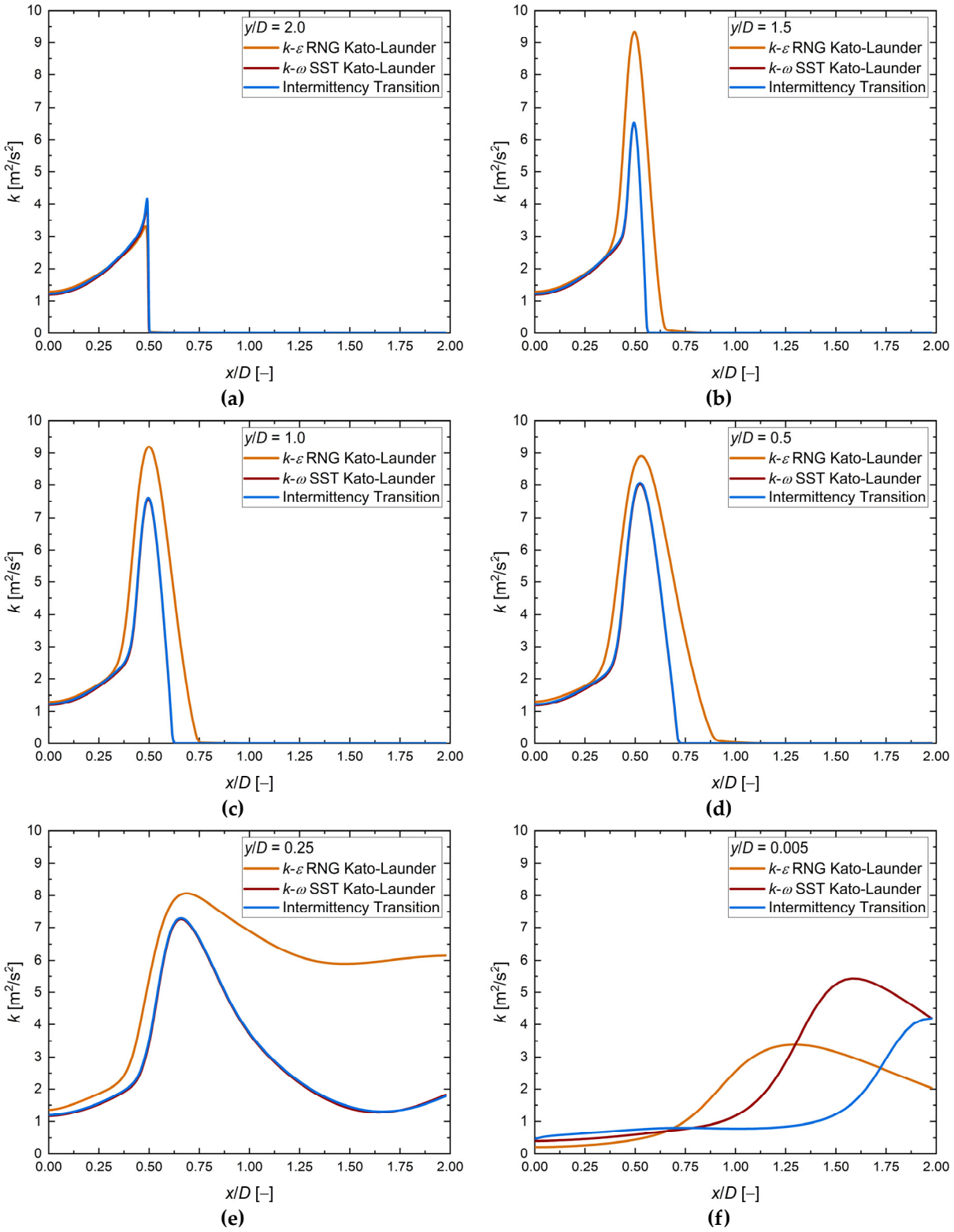

Figure S14. Turbulent kinetic energy profile development. $H/D = 2$, $D = 0.02$ m, Re = 23,000, (a) $y/D = 2.0$, (b) $y/D = 1.5$, (c) $y/D = 1.0$, (d) $y/D = 0.5$, (e) $y/D = 0.25$, (f) $y/D = 0.005$. y — vertical distance from the heated wall ($y/D = 0$ — heated wall, $y/D = 2.0$ — exit of the inlet channel), x — horizontal distance from axis ($x/D = 0$ — axis).

5. Comparison of the local Nusselt number distribution between the numerical analysis

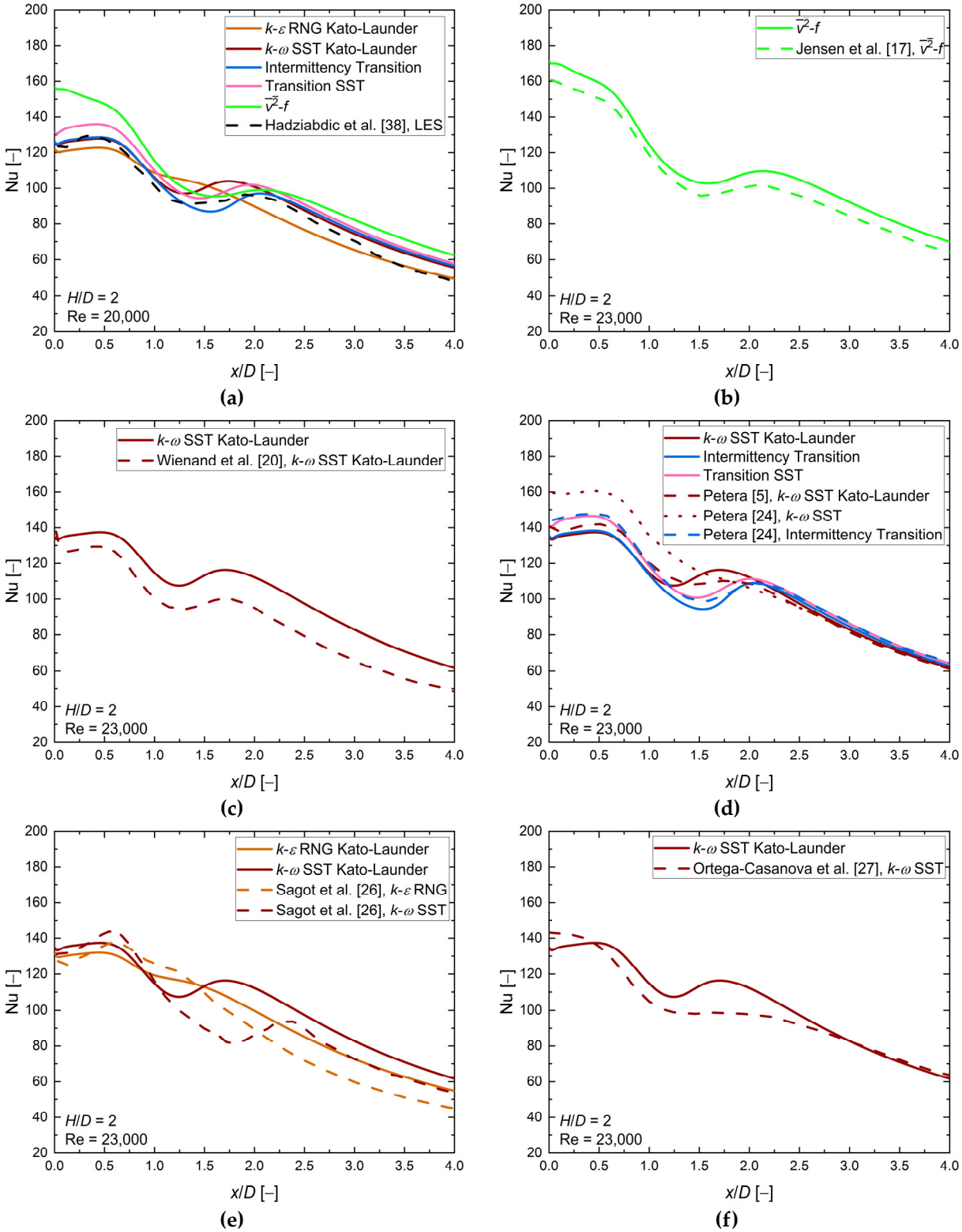

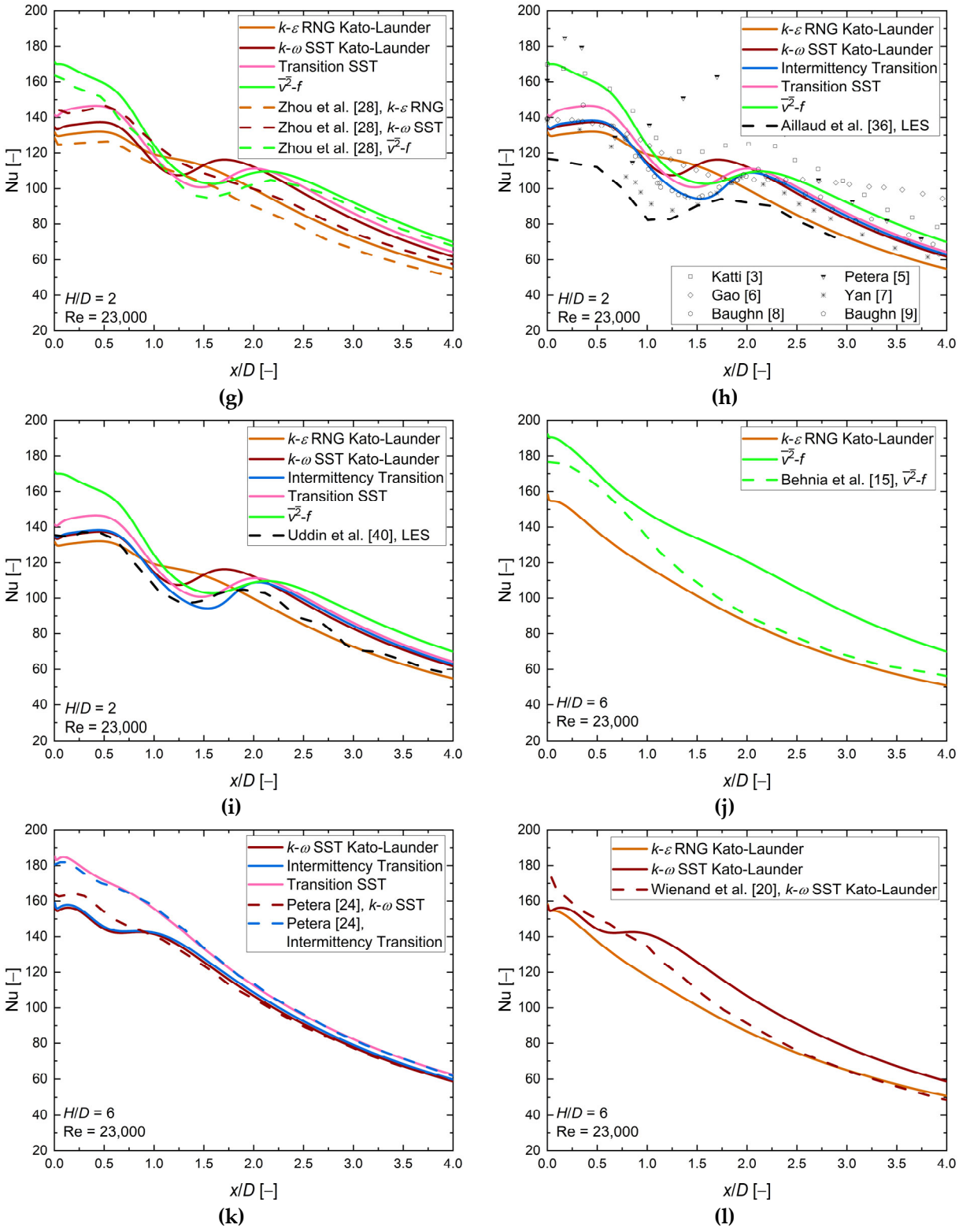

Figure S15. Comparison of the local Nusselt number distribution between numerical analyses. (a) — H/D = 2, Re = 20,000, (b) – (i) — H/D = 2, Re = 23,000, (j) – (l) — H/D = 6, Re = 23,000.